# First-Principles Study of Thermoelectric Effect in Two-dimensional Ferromagnet

| メタデータ | 言語: eng |
|---|---|
| | 出版者: |
| | 公開日: 2021-03-17 |
| | キーワード (Ja): |
| | キーワード (En): |
| | 作成者: |
| | メールアドレス: |
| | 所属: |
| URL | http://hdl.handle.net/2297/00061346 |

# Abstract

# First-Principles Study of Thermoelectric Effect in Two-dimensional Ferromagnet

二次元強磁性体における熱電効果の第一原理的研究

Graduate School of
Natural Science & Technology
Kanazawa University


Division of Mathematical and Physical Sciences



Student ID: 1724012009
Name : Rifky Syariati
Chief Advisor : Prof. Fumiyuki ISHII
Date of Submission : 22 October 2020

**Abstract**

We implemented first-principles calculations to elucidate the anomalous Nernst effect (transverse thermoelectric effect) of the half-metallic FeCl$_2$ monolayer. We investigated its thermoelectric properties based on the semiclassical transport theory including the effect of Berry curvature. If we assumed 10 fs for the relaxation time, the carrier-doping generates a large anomalous Nernst effect which was approximately 6.65 $\mu$V/K at 100 K. The origin of this large magnitude comes from large Berry curvature at the K-point of the hexagonal Brillouin zone. These results indicate that two-dimensional ferromagnetic half-metallic materials can potentially be applied in thermoelectric devices.

**Key words**: First-principles calculation, two-dimensional magnetic materials, thermolectric, anomalous Hall effect, anomalous Nernst effect

# 1 Introduction

Thermoelectric generation is a method to generate electricity from the heat. It is a clean conversion because it uses not only waste heat from such as motor vehicles, households, and factories but also heats from environmental heat sources. Thermoelectric generators are solid-state semiconductor devices that convert a temperature difference and heat flow into a useful DC power source. The basic building block of a thermoelectric generator is a thermocouple which is made up of one p-type semiconductor and one n-type semiconductor. The semiconductors are connected serially by a metal strip. Thermoelectric generator semiconductor devices employ the Seebeck effect to generate a voltage. This generated voltage generates electrical current and produces useful power at a load. However, there is a deficiency in the Seebeck energy conversion. The Peltier heat current will convey heat sometimes which degrading the conversion efficiency. Because of that, the researcher tries to resolve this problem by using the magnetic material which generating anomalous Nernst effect (ANE) in thermoelectric devices.

The anomalous Nernst effect (ANE) thermoelectric power generation attracts the researcher due to its flexible and simple structure and low generation cost in fabrication [1]. ANE offers for high flexibility degree in device design since when the temperature gradient is applied, the material length along the temperature gradient is not needed because the anomalous Nernst voltage increases with the transverse length normal to both the magnetization and the temperature gradient. Thus, thermoelectric devices based on the ANE can be adaptable with any heat source. So, the materials such as thin films and two-dimensional (2D) materials can be employed as the base in these devices. In the ANE case, the Ettingshausen heat current is generated by the electric current from the low-temperature side to the high-temperature side. This current increases the conversion rate efficiency, because Ettingshausen heat current and the electric current directions are perpendicular to each other [2].

The conversion efficiency of ANE thermoelectric materials is dependent on their anomalous Nernst coefficient (ANC). Using 2D materials is one of the solutions to this problem. For example, the EuO monolayer is shown that it possesses a large ANC [3, 4]. In 2D materials, the ANE is associated to the quantum anomalous Hall effect. AHC in the 2D system is influenced by the quantized anomalous Hall conductivity (AHC), which can be denoted by $\sigma_{xy} = \frac{e^2}{h}C$, where $C$ is Chern number. The quantized AHC was proved experimentally by Chang et al. [5] in a magnetically doped thin film of a topological insulator $(Bi, Sb)_2Te_3$. Their results suggest that it is possible to found a large ANC in 2D systems.

In this study, we investigated the thermoelectric properties of a half-metallic 1T-FeCl$_2$ monolayer with density functional calculations. We obtain that the 1T-FeCl$_2$ monolayer possesses high AHC, which generates a large ANC. The high AHC has resulted from the bands at the K-point of Brillouin zone near the Fermi level, where a large Berry curvature lies. In addition, the thermoelectric properties of the 1T-FeCl$_2$ monolayer can be tuned by charge doping. By this approach, we obtain a large ANC at the Fermi level. Based on this, it can be concluded that 2D magnetic half-metallic materials generate high ANC values.
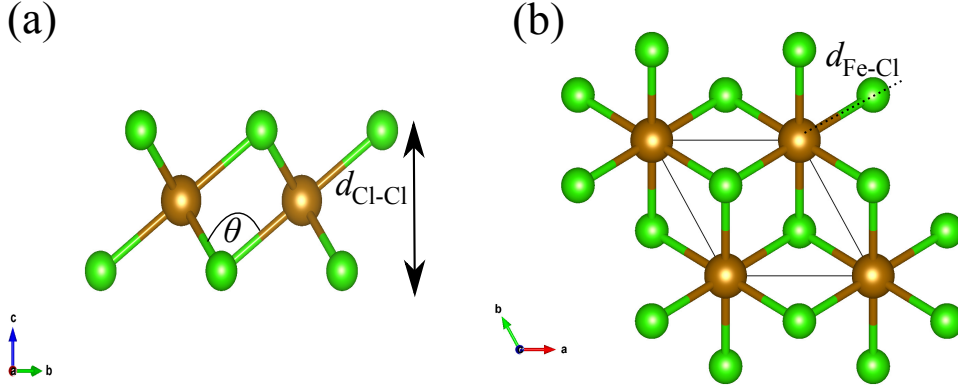
Figure 1: (a) Side and (b) top views of 1T-FeCl$_2$ monolayer structure. Brown and green spheres indicate Fe and Cl atoms, respectively. Structural parameters of 1T-FeCl$_2$ monolayer, namely, angle between Fe-Cl-Fe atoms, vertical distance of Cl-Cl atoms, and distance between Fe-Cl atom are represented by $\theta$, $d_{Cl-Cl}$, $d_{Fe-Cl}$, respectively.

## 2 Computational Method

The density functional theory calculation is applied by OpenMX code [6]. The generalized gradient approximation with the Perdew-Burke-Ernzerhof functional is used for treating the exchange-correlation potential [7]. The norm-conserving pseudopotentials and pseudo-atomic localized basis functions are employed. The wave functions are extended by using a linear combination of multiple pseudoatomic orbitals [8]. We specify the pseudoatomic orbitals as Fe6.0S-s2p3d3f1 and Cl7.0-s3p3d2 where 6.0 and 7.0 are the cutoff radius of Fe and Cl atom in the unit Bohr respectively, $S$ is soft pseudopotential, and radial function multiplicity of each angular momentum component is defined by the number after $s$, $p$, $d$, $f$ in the pseudoatomic orbitals format. We set the charge density cutoff energy at 500.0 Rydbergs and (20,20,1) k-point mesh for the self-consistent field calculations (SCFs). Moreover, the spin-orbit interaction (SOI) was included [9] for the noncollinear density functional calculations. The convergence during k-point sampling and the cut-off energies are checked. We optimized all the atomic positions and lattice parameters of the 1T-FeCl$_2$ monolayer using the eigenvector-following quasi-Newton algorithm until all the forces were smaller than $10^{-6}$ Hartrees/Bohr reached [10]. We also determined the lattice constant based on the total energy minimum.

The side view of the 1T-FeCl2 monolayer structure can be seen in Fig. 1(a) while Fig. 1(b) shows the top view of the 1T-FeCl2 monolayer. Both of the Fig. 1(a) and Fig. 1(b) show that Fe atom is encircled by six Cl atoms. Those figures also show the hexagonal lattice as the primitive cell of the 1T-FeCl2 monolayer, wherein the magnitude of the lattice constant ($\vec{a}$) is equal to that of $\vec{b}$ with the vacuum region c = 17.26 Å. The $\vec{a}$ of the 1T-FeCl$_2$ monolayer was 3.48 Å. The vertical distance between the Cl atoms ($d_{Cl-Cl}$) is 2.78 Åwhile the distance between the Fe and Cl atoms ($d_{Fe-Cl}$) is 2.44 Å. The angle of Fe-Cl-Fe ($\theta$) is 89.90°. These calculated parameters of monolayer were in good agreement with previous theoretical studies on FeCl$_2$[11, 12, 13, 14]. The calculated lattice constant for monolayer FeCl$_2$ were similar value to those of bulk FeCl$_2$, a=3.6 Å[15, 16].

The Wannier90 code was applied to construct maximally localized Wannier functions (MLWFs) based on the results of the DFT calculations for calculating the thermoelectric

properties [17]. The 22 Wannier bands are constructed within the range of -15 eV to 15 eV for outer window energy and -4 eV to 4 eV for inner window energy. The transport properties based on the MLWFs is computed by using the semiclassical Boltzmann transport theory [18] within constant relaxation time approximation, $\tau = 10$ fs, and k-point mesh (300,300,1). This method was used successfully to study the thermoelectric properties of skyrmion crystal and half-Heusler compounds [19, 3, 4].

# 3    Results and Discussions

The electronic band structure of 1T-FeCl$_2$ monolayer in the FM configuration is shown in the Figure 2 (a) and 2 (b). It can be seen that the minority states cross the Fermi level. On the other hand, the majority of states have a large gap. It indicates that the ground states of the 1T-FeCl$_2$ monolayer are half-metallic. The states near the Fermi level of the 1T-FeCl$_2$ monolayer were mostly composed by the 2p orbitals of the Cl atoms and the 3d orbital of the Fe atom, as shown in Fig. 2 (c). These states are investigated as anti-bonding states of Fe 3d and Cl 2p. According to the ligand field theory [20], the octahedral geometry of Cl atoms around a Fe atom leads to the splitting of the energy between the $d$ orbitals. This is ascribable to the electron-electron repulsion between the Fe and Cl orbitals.

The main component of $N$ consists of the pure Nernst coefficient ($N_0$), the pure Seebeck coefficient ($S_0$), the Hall angle ($\theta_H$). $S_0$ contributes to $N$ around 0.2% each. However, since the sign of $N_0$ and $\theta_H S_0$ are same at both 50 K and 100 K, $N_0$, and $\theta_H S_0$ weaken each other. If the chemical potential $\mu$ is tuned by carrier doping, $N$ can be increased as can be viewed from the rigid band approximation (RBA) in Fig. 3.

Fig. 3 describes the chemical potential dependences of the Nernst, $N$, coefficients of the 1T-FeCl$_2$ monolayer at 50 K and 100 K . According to it, the value of $N$ is small at $\mu$ = 0 at both 50 K and 100 K. Beside of that, a large value $N$ occurs at approximately $\mu$ = 0.16 eV, $\mu$ = 0.31 eV, and $\mu$ = 0.35 eV which denoted by peak 1, 2, and 3, respectively. By using self-consistent field carrier doping methods, the RBA calculation is quite well for 1T-FeCl$_2$. The role of pure Nernst and Seebeck effect in detail are presented in the dissertation.

The chemical potential dependence of the AHC ($\sigma_{xy}$) and the longitudinal electrical conductivity ($\sigma_{xx}$) with $\tau$ = 10 fs is exhibited in Fig. 4 for elucidating the properties of coefficients $N$. $\sigma_{xx}$ as a function of chemical potential influences the magnitude and sign of $S_0$. As shown in Fig. 4, $\sigma_{xx}$ shows a positive slope at energy values lower than $\varepsilon$ = -0.2 eV, which make $S_0$ demostrating a negative value. This is also occurred in the case for $N_0$. The magnitude and sign of $N_0$ rely on $\sigma_{xy}$ as a function of energy. If there is a slope at a energy in $\sigma_{xy}(\varepsilon)$, the $N_0$ will large around the energy. As stated from Mott's formula, which is $\alpha_{ij} = -\frac{(\pi k_B)^2}{3e} \frac{\partial \sigma_{ij}(\varepsilon)}{\partial \varepsilon} T \mid_{\varepsilon = \mu}$, the $N_0$ is affected by slope of $\sigma_{xy}$. The slope of $\sigma_{xy}$ on $\mu$ = -0.3 eV to $\mu$ = -0.1 eV, did not contributes to $N_0$ because $\sigma_{xx}$ is large at this point. However, the slope of $\sigma_{xy}$ around $\mu$ = -0.1 eV to $\mu$ = -0.18 eV gives large contribution for $N_0$. Moreover, the large of $N$ around $\mu$ = 0.3 eV and $\mu$ = 0.35 eV which denoted by peak 2 and 3 as presented on the Fig. 3 is not mainly originated from $\sigma_{xy}$. It is contributed by the $\sigma_{xx}$ which approaching to zero magnitude.

The sign change of $\sigma_{xy}$ can be associated with the band filling near the Fermi level. If the charge doping is given, the Fermi level will be shifted and it will alter the charge filling near Fermi level. The band filling effect on $\sigma_{xy}$ is shown in the Fig. 5(a). The
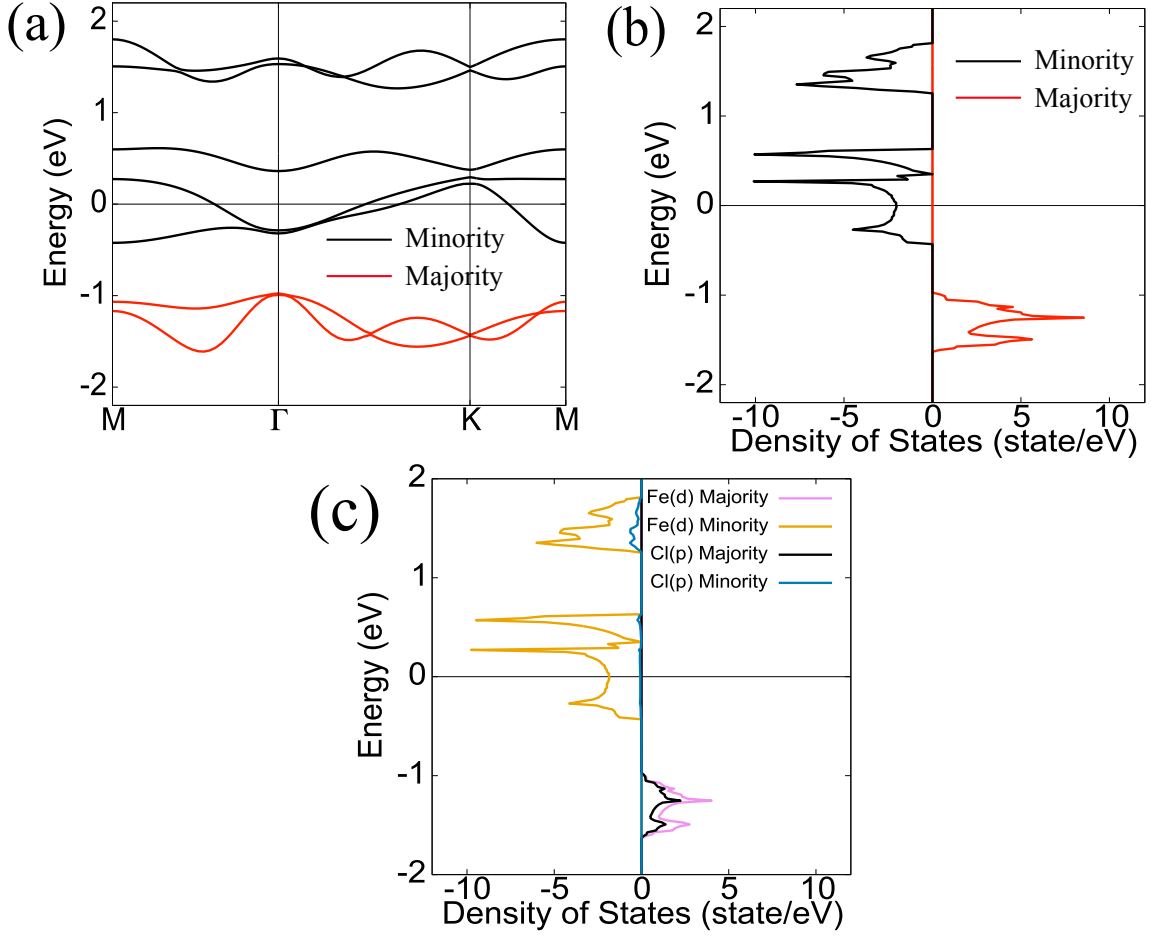
Figure 2: The electronic structure of ferromagnetic 1T-FeCl$_2$ monolayer which consists of spin-polarized (a) band structure and density of states where red and black lines indicate majority and minority states, respectively, and (c) projected density of states (PDOS).
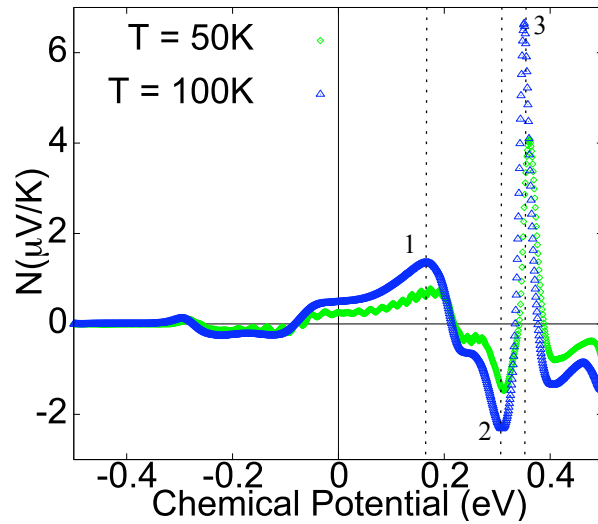


Figure 3: Chemical potential and temperature dependence of anomalous Nernst coefficient (ANC), $N$, at 0 K on 1T-FeCl$_2$ monolayer.
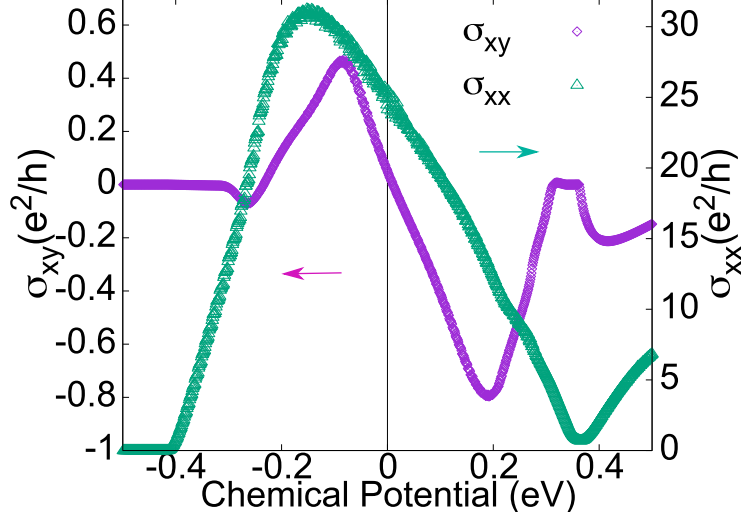
Figure 4: Chemical potential and temperature dependence of the AHC ($\sigma_{xy}$) and the longitudinal electrical conductivity ($\sigma_{xx}$) with $\tau = 10$ fs at 0 K.

blue band has a negative sign of $\sigma_{xy}$ and the red band has a positive sign of $\sigma_{xy}$ while the green band gives no contribution to the $\sigma_{xy}$. The total $\sigma_{xy}$ which marked by purple lines is calculated by the sum of red and blue band contributions. The detailed explanation of Berry curvature which is related to the red and blue band is shown in Fig. 5(b). Berry curvatures in the $\Gamma$-K line have a magnitude which is contributed by a red and blues band.
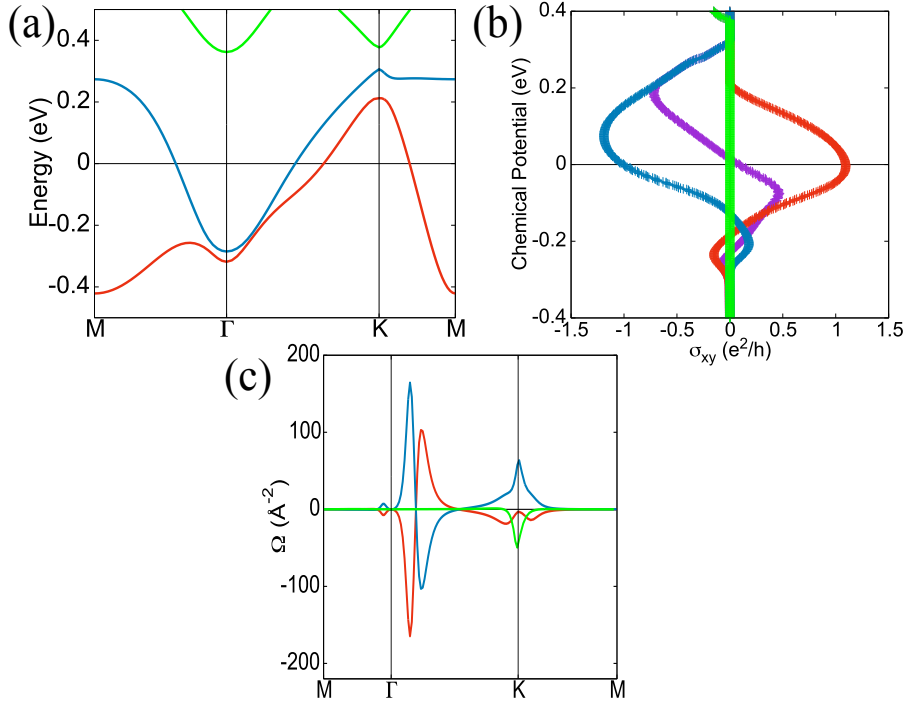


Figure 5: Band decomposition in the chemical potential dependence of (a) $\sigma_{xy}$ and (b) Berry curvature from band decomposition of 1T-FeCl$_2$ monolayer. Red and blue lines indicate the band contribution near Fermi level.

# 4 Conclusions

There are two origins of large anomalous Nernst coefficient (ANC) which can be reached in the 1T-FeCl2$_2$ monolayer based on the rigid band approximation (RBA). First, the ANC is reinforced by the pure Nernst and Seebeck coefficient. In this case, the slope of anomalous Hall conductivity gives a significant contribution to ANC. Second, the large ANC comes from near zero electrical conductivity although the pure Nernst and Seebeck coefficient are weakened each other. The maximum magnitude of ANC has a value as high as 6.65 $\mu$V/K for chemical potentials of 0.33 eV to 0.36 eV based on rigid band approximation (RBA). The high value of the ANC can be generated to the large Berry curvature, which is induced by the bands around the K-point of the Brillouin zone of the 1T-FeCl$_2$ monolayer. These results indicate that the ferromagnetic half-metallic 1T-FeCl$_2$ monolayer possesses high ANC magnitudes which can potentially be applied in thermoelectric devices.

# References

[1] Yuya Sakuraba. "Potential of thermoelectric power generation using anomalous Nernst effect in magnetic materials". In: *Scr. Mater.* 111 (2016), pp. 29–32.

[2] TC Harman and JM Honig. "Theory of galvano-thermomagnetic energy conversion devices. II. Refrigerators and heat pumps". In: *J. Appl. Phys.* 33 (1962), pp. 3188–3194.

[3] Yo Pierre Mizuta and Fumiyuki Ishii. "Large anomalous Nernst effect in a skyrmion crystal". In: *Sci. Rep.* 6 (2016), p. 28076.

[4] Yo Pierre Mizuta, Hikaru Sawahata, and Fumiyuki Ishii. "Large anomalous Nernst coefficient in an oxide skyrmion crystal Chern insulator". In: *Phys. Rev. B* 98 (2018), p. 205125.

[5] Cui-Zu Chang et al. "Experimental observation of the quantum anomalous Hall effect in a magnetic topological insulator". In: *Science* 340 (2013), pp. 167–170.

[6] Taisuke Ozaki et al. "www.openmx-square.org". In: ().

[7] John P. Perdew, Kieron Burke, and Matthias Ernzerhof. "Generalized Gradient Approximation Made Simple". In: *Phys. Rev. Lett.* 77 (18 Oct. 1996), pp. 3865–3868.

[8] T. Ozaki. "Variationally optimized atomic orbitals for large-scale electronic structures". In: *Phys. Rev. B* 67 (15 Apr. 2003), p. 155108.

[9] Gerhard Theurich and Nicola A Hill. "Self-consistent treatment of spin-orbit coupling in solids using relativistic fully separable ab initio pseudopotentials". In: *Phys. Rev. B* 64 (2001), p. 073106.

[10] Jon Baker. "An algorithm for the location of transition states". In: *J. Comput. Chem.* 7 (1986), pp. 385–395.

[11] Vadym V. Kulish and Wei Huang. "Single-layer metal halides MX$_2$ (X = Cl, Br, I): stability and tunable magnetism from first principles and Monte Carlo simulations". In: *J. Mater. Chem. C* 5 (2017), pp. 8734–8741.

[12] Engin Torun et al. "Stable half-metallic monolayers of $FeCl_2$". In: *Appl. Phys. Lett.* 106 (2015), p. 192404.

[13] Sherin A Saraireh and Mohammednoor Altarawneh. "Thermodynamic stability and structures of iron chloride surfaces: A first-principles investigation". In: *J. Chem. Phys.* 141 (2014), p. 054709.

[14] Yulin Feng et al. "Robust half-metallicities and perfect spin transport properties in 2D transition metal dichlorides". In: *J. Mater. Chem. C* 6.15 (2018), pp. 4087–4094.

[15] C Vettier and WB Yelon. "The structure of $FeCl_2$ at high pressures". In: *J. Phys. Chem. Solids* 36 (1975), pp. 401–405.

[16] MK Wilkinson et al. "Neutron Diffraction Investigations of the Magnetic Ordering in $FeBr_2$, $CoBr_2$, $FeCl_2$, and $CoCl_2$". In: *Phys. Rev.* 113 (1959), p. 497.

[17] Arash A Mostofi et al. "An updated version of wannier90: A tool for obtaining maximally-localised Wannier functions". In: *Comp Phys. Comm.* 185.8 (2014), pp. 2309–2310.

[18] John M Ziman. *Principles of the Theory of Solids*. Cambridge university press, 1979.

[19] Susumu Minami et al. "First-principles study on thermoelectric properties of half-Heusler compounds CoMSb (M= Sc, Ti, V, Cr, and Mn)". In: *Appl. Phys. Lett.* 113 (2018), p. 032403.

[20] F. Albert Cotton. "I - Ligand field theory". In: *J. Chem. Educ.* 41 (1964), p. 466.

## 学位論文審査報告書（甲）

1．学位論文題目（外国語の場合は和訳を付けること。）

First-Principles Study of Thermoelectric Effect in Two-dimensional Ferromagnet

（二次元強磁性体における熱電効果の第一原理的研究）

2．論文提出者　（1）所　属　　　数物科学　専攻

　　　　　　　　（2）氏　名　　　Rifky Syariati（りふきい　しゃりあてい）

3．審査結果の要旨（600〜650字）

Rifky Syariati 氏の学位論文について、審査委員で提出された論文と口頭発表による詳細な検討を行った後、8月5日に学位論文公聴会を実施した。公聴会の後、審査委員で審議を行った。近年、物質を究極まで薄くした数原子層の二次元強磁性体が発見され、加工のしやすさ等から、様々な形態の熱源による熱電効果（異常ネルンスト効果）を用いた排熱有効利用へ応用可能な熱電材料として期待されている。しかし、二次元強磁性体を熱電材料として用いるために重要な、高い磁気転移温度、二次元面に面直方向の磁化を示す物質が実験的に発見されておらず、その熱電効果はほとんど調べられてこなかった。Rifky Syariati 氏は層状の磁性体である $FeCl_2$ の単層について、電子状態計算を行い、強磁性相の異常ネルンスト効果を調べ、$FeCl_2$ が熱電材料の候補となりうることを示した。ベリー曲率(波数空間での仮想磁場)を考慮したボルツマンの輸送方程式によって異常ネルンスト係数を見積もり、電子ドープを仮定すると、$FeCl_2$ はこれまで報告されている最大値にせまる異常ネルンスト係数を示す可能性があることを明らかにした。そして、その大きな異常ネルンスト係数の起源がフェルミ準位を横切る二つのバンドにおける巨大なベリー曲率であることを明らかにした。以上の様に、Rifky Syariati 氏の研究は二次元強磁性体の熱電材料としての可能性を明らかにした重要な研究であると判断し、合格と結論した。

4．審査結果　　（1）判　定（いずれかに○印）　　（合　格）・　不合格

　　　　　　　　（2）授与学位　　博　士（　理学　）